

# The aperture and precision of the Auger surface array

**M. Ave<sup>1</sup>, J. Lloyd-Evans<sup>1</sup>, A. A. Watson<sup>1</sup>, for the The Pierre Auger Observatory Collaboration<sup>2</sup>**

<sup>1</sup>Department of Physics and Astronomy, University of Leeds, Leeds LS2 9JT ,UK

<sup>2</sup>Observatorio Pierre Auger, Av. San Martin Norte 304, (5613) Malargüe, Argentina

**Abstract.** The expected sensitivity of the water Cerenkov detector array of the southern Auger Observatory site is described by calculations of the energy and zenith angle dependent aperture function ( $A(E,\theta)$  km<sup>2</sup> sr). The calculations are based, whenever possible, on the forms of the lateral distribution and shower size attenuation that have been empirically determined from previous giant air shower arrays. The uncertainties arising from the extrapolation to distances beyond 2 km and to extreme zenith angles ("horizontal air showers") are discussed. Particular attention is paid to the effect of trigger schemes on the acceptance "turn-on" at the array threshold and the energy dependent station multiplicity. Finally the aperture calculations are compared with estimates provided by simple MC calculations.

## 1 Introduction

The Auger Southern Observatory surface detector array will consist of 1600 water Cerenkov detector stations (each 10 m<sup>2</sup> x 1.2 m deep) on a hexagonal grid of 1,500 m spacing. The array covers a ground area of approximately 3000 km<sup>2</sup> at a mean altitude of 875 g cm<sup>-2</sup> (1200 m) near Malargüe in Mendoza County, Argentina (lat = -35.2°, long = -69.2°). This paper outlines the performance characteristics of the surface detector alone ; the performance of the Fluorescence Detector and the combined ("hybrid") detector are described in the accompanying papers of the Auger Collaboration.

In section 2 we present estimates of the measurement precision of two important shower reconstruction variables : the arrival direction, and the energy, together with the energy dependent triggering efficiency and anticipated shower detection rates for the full array.

The performance of the surface detector engineering array, a 40 station subgroup of the full array currently nearing completion, is presented in section 3.

Preliminary estimates of the potential for a significantly

enlarged aperture for showers at high zenith angles ( $> 60^\circ$ ) is given in section 4, with a discussion on the limitations of current estimates imposed by uncertainties in reconstruction at large zenith angles.

## 2 Shower Reconstruction and Aperture

A full description of the procedures used to estimate the precision achievable using the surface detector alone is given in Billoir [Billoir (2000)]. Briefly, a Monte Carlo (AIRES plus QGSJET) library of 1000 showers covering energies above 10<sup>19</sup> eV, zenith angles up to 60° and three different primary species (proton, iron and photons) are sampled to generate water Cerenkov detector signal densities and arrival times on a grid of detector stations with 1.5 km spacing.

Care has been taken to keep biases and artificial fluctuations that are induced by the inevitable Monte Carlo thinning process to a minimum ; a thinning level of 10<sup>-7</sup> has been used and a local detector station sampling method applied [Billoir (2000)]. A simple model of water Cerenkov signal generation within each station is then applied and the resulting station signal, together with the station trigger time are passed to a shower reconstruction program if at least  $n$  non colinear stations record signals above a preset threshold. The station signal is integrated over 10 microseconds and expressed in units of 100 pe, which corresponds roughly to 1 vertical equivalent muon (vem). The station trigger time is set when the signal exceeds 2 pe. The number of stations and signal threshold needed for reconstruction have been set in the present work to a multiplicity of 5 and 4 vem respectively. The multiplicity allows for some redundancy in shower parameter fitting and the threshold is comfortably achievable within the station data rate limit of 20 Hz.

### 2.1 Arrival direction reconstruction

An initial fast estimate of the shower direction is obtained by fitting a plane shower front to the three largest station signals and a "weighted center of gravity" estimate of the core lo-

Correspondence to: M. Ave (ave@ast.leeds.ac.uk)

$\theta$	Proton/Iron	Photon
All Energies	$E > 10^{20}$ eV	
20	1.1	0.6
40	0.6	0.5
60	0.4	0.3
80	0.3	0.2
		1.0

**Table 1.** The space angle containing 68 % of reconstructed directions

cation is made. Subsequent arrival direction fitting applies a weighted least squares fit to the station times, resulting in the angular reconstruction accuracy given in Table 1. The angular accuracy is quoted for the opening space angle containing 68% of the reconstructed directions, as a function of zenith angle.

The reconstruction is slightly better for iron than for proton initiated showers primarily because of their larger muon to electromagnetic ratio; the tabled values assume an equal mix and show that the resolution is better than 1.1 degrees for all energies, improving rapidly with increasing zenith angle up to 60° and improving substantially for larger events above  $10^{20}$  eV (largely because of the greater number of triggered stations). Photon initiated showers are not as well reconstructed, especially at small zenith angles, primarily because retarded shower development (including the LPM effect) restricts the shower "footprint" at ground level. It should be noted that photon initiated showers will be distinguishable from nucleon initiated showers in the characteristic shower front curvature, signal risetime and muon content and that photons that convert (on the geomagnetic field) are reconstructed with higher precision [Bertou (2000)].

## 2.2 Core Location reconstruction

A refined core location estimation is made by fitting the station signal densities to the expected lateral distribution function (ldf) with the core location and shower density at a reference distance ( $\rho(1000\text{m})$ ) as free parameters. A number of ldf parametrisations have been examined (see [Billoir (2000)] for details), including the ldf obtained from fits to archival Haverah Park data adapted to this energy range  $\rho(r) = k r^{-(\eta+r/4000\text{ m})}$ , where  $k$  is a normalization constant, and  $\eta$  is given by  $\eta = 3.98 - 1.29 \sec \theta$ . This function is flattened by a factor  $(r/800)^{1.03}$  when  $r > 800$  m. In the present work a fixed relative station density uncertainty of 20 % has been applied to all stations with  $r < 2000$  m (rising at larger distances - see [Billoir (2000)]). Further work is being done to investigate more detailed parametrisations of the signal density uncertainty.

## 2.3 Energy Resolution

The zenith angle dependent relation between the fitted density at 1000 m and the input primary energy obtained from Monte Carlo is used to estimate the energy resolution.

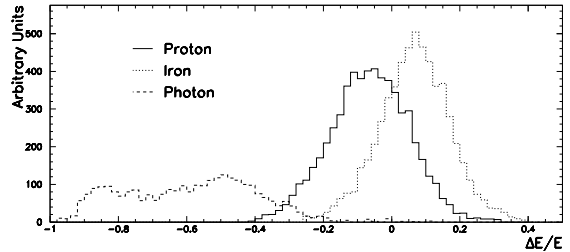


**Fig. 1.** Relative uncertainty on energy for proton (solid), iron (dashed) and photon (dotted) simulated showers, using the modified HP lateral distribution function to fit the core position and  $\rho(1000)$ . In this analysis the energy of photon initiated events is systematically underestimated because an energy conversion for a proton/iron composition is assumed.

The measured dispersion in  $\rho(1000)$  for fitted showers results in an energy resolution comprising of three parts : a statistical part arising from angle and density measurement uncertainties, a statistical part from shower-to-shower development fluctuations, and a systematic component due to shower model uncertainties relating to the longitudinal shower development and the nature of the primary. The relation between  $\rho(1000\text{ m})$  and primary energy was obtained by averaging the conversion factor for proton and iron primaries. Fig. 1 shows the resulting relative dispersion in energy.

With the model adopted here, the rms energy resolution is estimated to be 12 % averaged over all energies (assuming a proton/iron primary mixture), falling to 10% above an energy of  $10^{20}$  eV. About 6% of the uncertainty at high energies arises from measurement errors, and the rest (in quadrature) from shower-to-shower fluctuations. The systematic error arising from SD reconstruction alone amounts to about 10%, but improves substantially with hybrid event reconstruction.

## 2.4 Trigger efficiency, aperture and detection rates

The limiting aperture for the full southern observatory array and for zenith angles  $< 60^\circ$  is  $7350 \text{ km}^2 \text{ sr}$ . The resulting trigger efficiency and anticipated detection rates are provided in Table 2. It should be emphasized that the detection rate becomes increasingly uncertain above  $5 \cdot 10^{19}$  eV. In the table

$E_0(\text{EeV})$	Trigger efficiency	Detection rate
1.	0	0
3.	0.3	15000
10.	0.98	5150
20.	1.	1590
50.	1.	490
100.	1.	$\sim 100^*$
200.	1.	$\sim 32$
500.	1.	$\sim 10$

**Table 2.** Trigger efficiency and detection rate per year. \* The detection rate becomes increasingly uncertain above  $5 \cdot 10^{19}$  eV (see text).

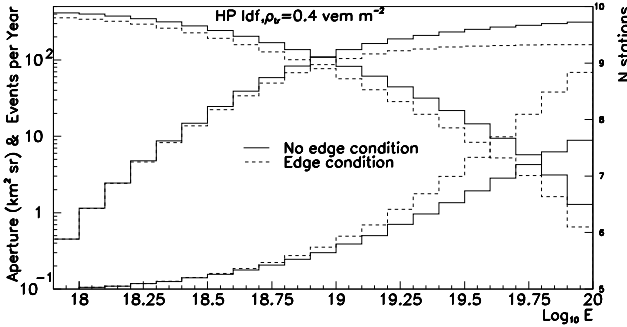


**Fig. 2.** The aperture, detection rate and station multiplicity as a function of energy for the engineering array. The edge condition applies an additional boundary condition (see text). The modified HP LDF and the spectrum given in [Nagano (2000)] is used for the calculation.

the rate is estimated assuming the AGASA [Takeda (1998)] spectrum and a 100 % reconstruction efficiency. Using the reference spectrum of [Nagano (2000)], for example, the estimated rate above  $10^{20}$  eV is nearer 70 events per year.

### 3 Aperture of the Engineering Array

Simulations have been performed to assess the performance of the first phase of the Auger Surface Detector consisting of a 40 detector engineering array currently under construction. In this first phase shower parameters can be measured with a similar precision to that discussed in the section 2, but at much reduced detection rate, because the station multiplicity of even the largest events is small in comparison with the array size.

Events falling near the array boundary however are less well reconstructed , so we have applied an additional trigger condition : the largest recorded signal must not be in a station on the array boundary. Fig. 2 shows the effect of this condition on the resulting aperture, detection rate and the multiplicity. The calculation was performed for zenith angles  $< 60^\circ$  and using the modified HP LDF described in the previous section.

It should be emphasized that the predicted aperture and rates are sensitive to the assumed LDF at large core distances: for example at  $10^{19}$  eV an uncertainty of at least 30% can arise from differences of the assumed LDF.

The aperture is also sensitive to the applied station trigger level, especially near the array energy threshold. The level adopted throughout this paper is  $0.4 \text{ vem m}^{-2}$  so that the operationally single station trigger rate is kept below 20 Hz. As an example Fig. 3 shows the effect of varying this trigger level on the engineering array aperture and station multiplicity.

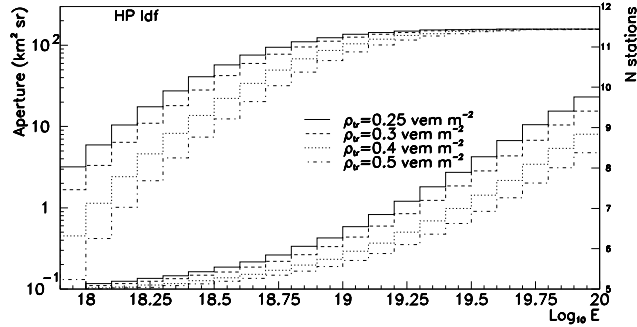


**Fig. 3.** The effect of the different station trigger levels to the aperture and multiplicity for the engineering array. The level adopted in this paper is  $0.4 \text{ vem m}^{-2}$ .

### 4 Extension to high zenith angles

The proposal to detect neutrino induced events by studying horizontal showers [Capelle (1998)] has led to an investigation of the capability of Auger to detect hadronic induced showers at large zenith angles. The electromagnetic part of the air showers induced by inclined cosmic rays is indeed absorbed before reaching ground level, but the muonic content of such showers propagates practically unattenuated to ground level. The muon density patterns at ground are however greatly affected by the deflection of the muons in the Earth's magnetic field.

If these showers can be reconstructed they provide a significant increase in the aperture of the array and may improve mass composition studies [Ave (2000a)].

Details of the modeling under the influence of the Earth's magnetic field are given in [Ave (2000b)]. Here we predict the expected rate for the Auger Surface Array above  $60^\circ$ .

In the present work we consider primary protons and QGSJET [Kalmykov (1997)] as the high energy interaction model. To account for the detector response to muons of different energy and impact angle the GEANT program [Brun (1993)] is used. The simulation includes the effects of direct light and muon interactions in the water detectors. The electromagnetic component of the inclined showers has been modelled with Monte Carlo simulations using AIRES [Sciutto (1999)]. We have generated simulated events in the energy range  $10^{18.5}\text{--}10^{21}$  eV, in the zenith angle range  $60^\circ\text{--}89^\circ$ , with a trigger condition of 5 stations with a density larger than  $0.4 \text{ vem m}^{-2}$ . For each simulated event the densities at each detector are fluctuated according to Poisson fluctuations in the number of muons, and also for the large fluctuations in the detector response due to direct light. The shower parameters are then reconstructed fitting the densities at the stations to the predicted densities given by the muon density maps with a likelihood method. An example of a reconstructed event is shown in Fig. 4. The asymmetry in the density pattern due to the geomagnetic field is apparent.

We have estimated the detection rate as a function of primary energy integrating over all zeniths and azimuths, using the representation of the energy spectrum of Nagano (2000).

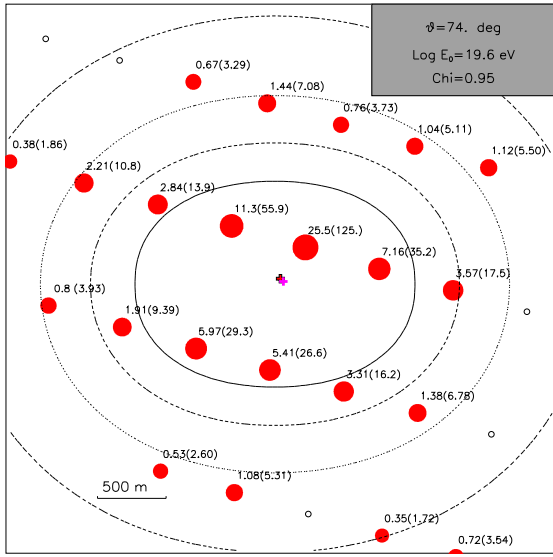


**Fig. 4.** Density map of a proton initiated event of  $10^{19.6}$  eV at a zenith angle of  $74^\circ$  in the plane perpendicular to the shower axis. Recorded muon densities are shown as circles with radius proportional to the logarithm of the density. The positions of the best-fit core and the *true* core are indicated by a star. Densities in  $\text{vem m}^{-2}$  are marked and, in brackets, the actual number of horizontal muons that produced each signal. The y-axis is aligned with the component of the magnetic field perpendicular to the shower axis. Contour levels for 2, 5, 10 and 20 muons per station are shown.

Fig. 5 shows the results. The continuous line represents the integral spectrum, using the *true* energy, of the events that trigger the array, and the dash line represents the reconstructed spectrum. The difference in normalization is due to quality cuts made to the reconstructed events. A difference in the slope of the spectrum is also apparent and is consistent with the improvement of the energy resolution at higher energies. Two factors contribute to the energy resolution calculated for this work: the variation of the number of muons at ground due to shower to shower fluctuations (20 %) and the measurement error reconstruction (which evolves from 30 % at  $10^{19}$  eV to 12 % at  $10^{20}$  eV). The number of expected events per year, assuming proton composition, is  $\sim 1000$  above  $10^{19}$  eV and  $\sim 18$  above  $10^{20}$  eV.

Fig. 5 also shows the multiplicity of detectors above  $0.4 \text{ vem m}^{-2}$  as a function of energy. For a given energy the multiplicity is much larger than for vertical showers. Two factors contribute to this effect: the reduction of the array spacing in the shower plane, and the flatter density profile of horizontal air showers compared to vertical.

It should be remarked that no attenuation of the shower across the array has been taken into account. As it is shown in [Ave (2000b)], such attenuation is only relevant at extreme zenith angles,  $\sim 87^\circ$ . In fact, the attenuation in horizontal air showers should be less important than in the vertical case. The main reason for this is that in the vertical direction the signal is dominated by electromagnetic particles, while in the horizontal direction the signal at ground level is dominated by

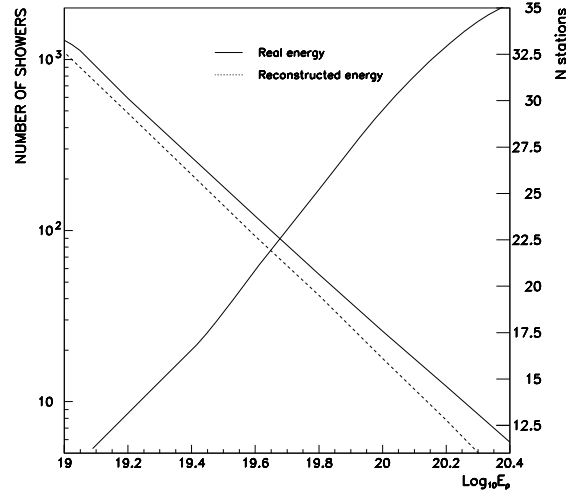


**Fig. 5.** Integral spectrum of events that trigger the Auger Surface Array, before and after energy reconstruction. The variation of the multiplicity in the number of stations is also shown.

high energy muons.

## Acknowledgements

We thank R.A. Vazquez and E. Zas for helping us to implement the model for geomagnetic deflections of muons at large zenith angles.

## References

- Kalmykov N, Ostapchenko S, Pavlov A I, Nucl. Phys. B 52B (1997) 17
- GEANT, Detector Description and Simulation Tool, CERN, Program Library CERN (1993)
- Nagano M., Watson A.A., Rev. Mod. Phys. **72** (2000) 689 and refs. therein.
- Capelle J., Cronin J.W., Parente G., and Zas E., Astropart. Phys. **8** (1998) 321.
- Ave M., Hinton J.A., Vazquez R.A., Watson A.A., and Zas E., Phys. Rev. Lett. **85** (2000a) 2244-2247 .
- Ave M., Vazquez R.A., and Zas E., Astropart. Phys. **14** (2000b), 91-107
- Aires: A System for Air Shower Simulation, S.J. Sciutto, Proc. of the XXVI Int. Cosmic Ray Conf. Salt Lake City (1999), vol. 1, p. 411-414; S.J. Sciutto preprint archive astro-ph/9911331.
- Takeda M. *et al.*, Phys. Rev. Lett. **81** (1998) 163.
- Billoir P., GAP note 2000-025.
- Bertou X., Billior P., and Dagoret-Campagne S., Astropart. Phys. **14** (2000) 121.